Wireless Pers Commun (2018) 103:761–772
https://doi.org/10.1007/s11277-018-5475-1

Image Adaptive Denoising Based on Nonsubsampled Contourlet Transform

Peng Wu[1] · **Baokun Wang**[1]

Published online: 7 February 2018

Abstract In this paper, researching the correlation property of congenetic subband coefficients of Nonsubsampled Contourlet Transform (NSCT), and proposing a new adaptive denoising theory. This theory combines the excellent shift-invariant of NSCT with the correlation property of congenetic subband coefficients in image denoising. The correlation property contains the entire relational correlation value of the congenetic subband coefficients, and the grey correlation value in single coefficient of the congenetic subband coefficients of the NSCT. According to the correlation property of congenetic subband coefficients, the new algorithm can automatically identify the strong edges, weak edges and noise in the noisy image, and then it can filter the noise and preserve the strong edges and weak edges at certain degree. The experiment results are provided to compare with the elegant non-local means method, which show that the theory proposed in this paper has good effect.

Keywords Adaptive · Nonsubsampled Contourlet Transform · Denoising · Correlation property · Congenetic subband coefficients

1 Introduction

Image denoising is a very important technology field and is also an important mission for further processing of image such as feature extraction, segmentation, texture analysis and so on. Processing the noise image directly to eliminate noise will lead to lose detail and texture characteristics of image and even reduce the contrast ratio of image. In order to solve this problem, the image denoising based on multiscale and multidirection has been developed.

✉ Peng Wu
wupeng@nefu.edu.cn

[1] College of Mechanical and Electronic Engineering, Northeast Forestry University, Harbin, China

Wavelet transform is the most successful "multiscale" and "multidirection" analysis method in twentieth century, which has been used in all kinds of signal and image analysis applications such as peak detection [1] in electrophoregram for separation science. Wavelet transform is also an efficient tool for image denoising [2, 3]. The wavelet transform has been developed in image denoising field. But because the wavelet basis is different dimensional square, when the resolution ratio elaborate degree increases, the size of square diminishes to be "point" at last to approach singularity curve. Wavelet transform just can decompose the image into four images in every decomposition; They are approximation and horizontal, vertical and diagonal details respectively. The wavelet transform has limited direction, which can't express singular high-dimensional function that contains line and surface sparsely and well. With the developing of multiscale transform technology, Minh N. Do and Martin Vetterli proposed Contourlet transform [4], which is a "real" two-dimension expressive method. Contourlet transform uses "long strip" basis to approach curve flexibly and changefully, which overcomes the imperfection that wavelet transform only has three directions. Every scale of Contourlet transform can be decomposed into different number and flexible direction basis, producing lots of multi-scale and multi-direction frequency sub-bands which contain edge detail information and texture characteristics. Contourlet transform can realize any scale and any direction decomposition. So, the Contourlet transform is a good choice for image denoising [5].

In addition, due to downsamplers and upsamplers in both the Laplacian pyramid and the direction filter bank, the Contourlet transform is not shift-invariant. When using Contourlet transform for image denoising, this will lead to pseudo-Gibbs phenomenon. In order to eliminate pseudo-Gibbs, Arthur L. da Cunha proposed the Nonsubsampled Contourlet Transform (NSCT) [6]. The NSCT [7] is a flexible and efficient transform target application for denoising when the redundancy is not the major issue. The NSCT is a fully shift-invariant, multiscale, and multidirection expansion that has a fast implementation.

2 Nonsubsampled Contourlet Transform

2.1 Nonsubsampled Pyramid

The multiscale property of the NSCT is obtained from a shift-invariant filtering structure that achieves a subband decomposition similar to that of the Laplacian pyramid. This is achieved by using two-channel nonsubsampled 2-D filter banks. Figure 1 illustrates the nonsubsampled pyramid decomposition with three stages.

The filters for subsequent stages are obtained by upsampling the filters of the first stage. The nonsubsampled pyramid decomposition can be obtained by removing the downsamplers and upsamplers in the Laplacian pyramid and then upsampling the filter accordingly. So, the nonsubsampled pyramid decomposition is different from the Laplacian pyramid decomposition of Contourlet transform. The multiscale decomposition of nonsubsampled pyramid is not the geometry multiscale decomposition but the multiscale decomposition of frequency plane. The frequency plane is decomposed into different scale frequency subbands as seen in Fig. 1b. And Fig. 1a shows the process of nonsubsampled pyramid decomposition. This decomposition process is invertible. If image x is decomposed into different scale frequency subbands on frequency plane, the image x can be reconstructed, using the process as seen in Fig. 2. H and G are the analysis and synthesis filter respectively.

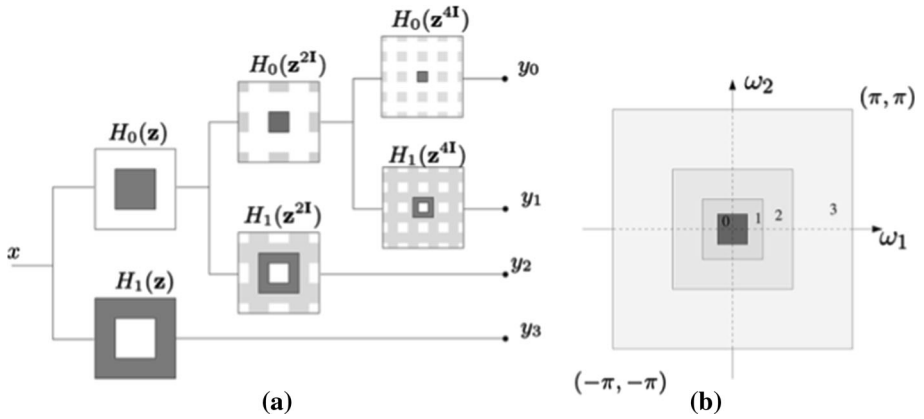

Fig. 1 **a** Three-stage pyramid decomposition. The lighter gray regions denote the aliasing caused by upsampling. **b** Subbands on the 2-D frequency plane

Fig. 2 Pyramid nonsubsampled filter bank

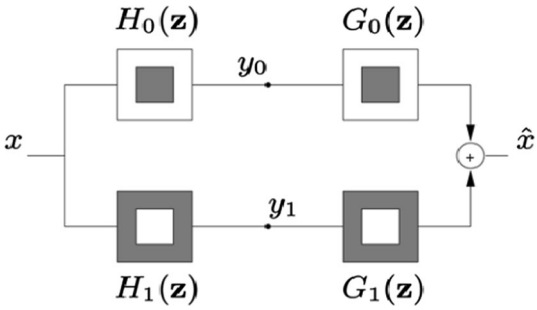

2.2 Nonsubsampled Directional Filter Bank (NSDFB)

The NSDFB is constructed by eliminating the downsamplers and upsamplers in the DFB. This is done by switching off the downsamplers and upsamplers in each two-channel filter bank in the DFB tree structure and upsampling the filters accordingly, which results in a tree composed of two-channel NSFBs. The NSDFB splits the 2-D frequency plane into directional wedges. This process can be illustrated in Fig. 3.

NSDFB can split the frequency subbands generated by the nonsubsampled pyramid into directional wedges that contain any number and any direction. The Fig. 3a shows the structure that splits the frequency subband x into four directions, and the Fig. 3b is the corresponding direction decomposition on the subband frequency plane. NSDFB is different from the DFB of Contourlet transform, and NSDFB just realizes the direction decomposition on the subband frequency plane. NSDFB just works on frequency field. The direction decomposition of frequency subband is also invertible. If the frequency subband x is decomposed into direction subbands, the frequency subband x can be reconstructed as the process showed in Fig. 4.

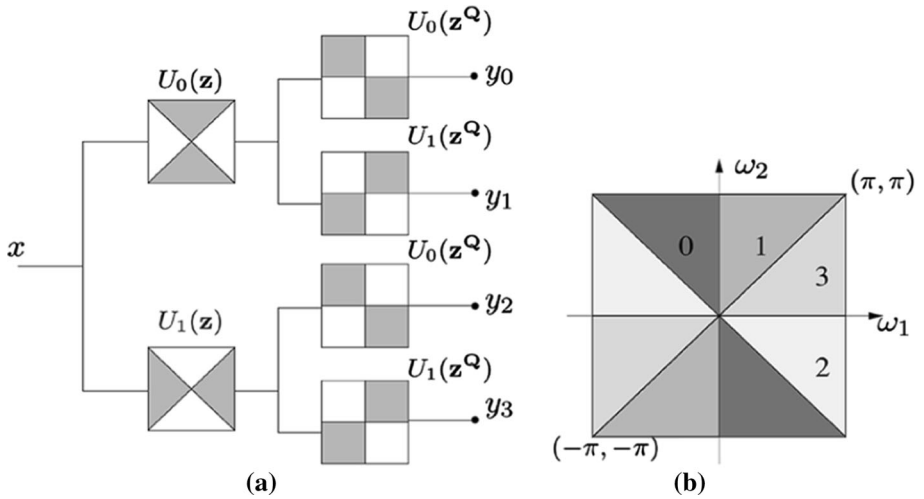

Fig. 3 **a** Four-channel nonsubsampled directional filter bank. **b** Corresponding frequency decomposition

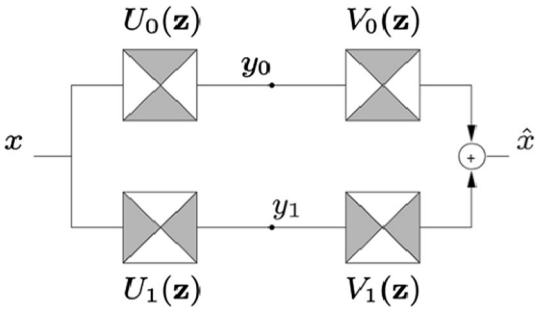

Fig. 4 The NSDFB with fan filters

2.3 Combining the Nonsubsampled Pyramid and Nonsubsampled Directional Filter Bank in the NSCT

The NSCT is constructed by combining the nonsubsampled pyramid with the NSDFB. Image x is processed by the nonsubsampled pyramid, generating the multiscale frequency subbands. And then these multiscale frequency subbands are processed by the NSDFB, generating the multiscale and multidirection frequency subbands, which realizes the multiscale and multidirection decomposition. The entire process can be seen in Fig. 5.

Figure 5 is the overview of the NSCT. The 2-channel NSFBs in the nonsubsampled pyramid and NSDFB are invertible, then clearly the NSCT is invertible. Due to the NSCT consists of two shift-invariant parts: a nonsubsampled pyramid structure and a nonsubsampled DFB structure, so, the NSCT is also shift-invariant. The NSCT is flexible, which allows any number of 2^l directions in each scale. In addition, the NSCT can satisfy the anisotropic scaling law, a key property in establishing the expansion nonlinear approximation behavior. This property is ensured by doubling the number of directions in the NSDFB expansion at every other scale. So, as seen above, the NSCT has larger redundancy than the Contourlet transform.

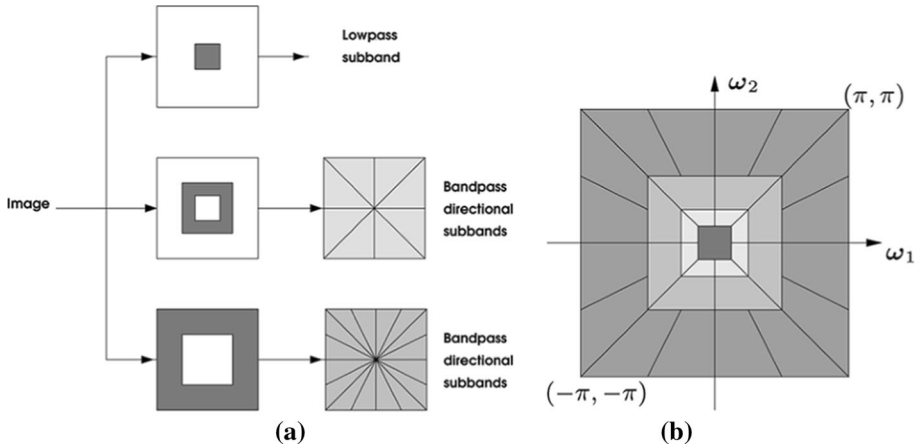

Fig. 5 **a** The NSFB structure that realizes the multiscale and multidirection decomposition. **b** The corresponding multiscale and multidirection frequency subbands frequency plane

3 Congenetic Subband Coefficients

As the discussion above, multiscale and multidirection decomposition is not the geometry multiscale or multidirection decomposition, but the frequency plane decomposition. The geometry size is the same, so each point of the subband coefficients of the NSCT corresponds to the point which has the same spatial location in the original image. Although all the subband coefficients have the same size, the pixel points in the same spatial location may have different grey value among each other. As the discussion above, all of the subband coefficients of the NSCT are relational.

According to the relational property, the pixels in all the subband coefficients of the NSCT can be classified into three categories: strong edges, weak edges and noise. The strong edges are the pixels that have large magnitude coefficients in all the subbands of the NSCT; the weak edges are the pixels which have large magnitude coefficients in intra-scale some directional subbands and small magnitude coefficients in intra-scale left directional subbands; the noise are the pixels that they have small magnitude coefficients in all of the subbands of the NSCT. Then how to use the relational property to identify the pixel categories is important. The traditional theory just considers the relational property of the intra-scale subband coefficients of the NSCT. In recent years, many researchers just study the relational property of the intra-scale and neighbouring inter-scale subband coefficients of the NSCT [8, 9].

The congenetic subband coefficients of the NSCT, which is proposed in this paper, have strong relational property. Figure 3a is the two level direction decomposition on the scale image x. For the further analysis, discussing the process of the three level direction decomposition on the scale image x: The first level direction decomposition, image x can generate direction subband coefficients v_0 and v_1. The second level direction decomposition, as seen Fig. 3a, v_0 can generate the direction subband coefficients y_0 and y_1; v_1 can generate the direction subband coefficients y_2 and y_3. The third level direction decomposition, y_0,y_1,y_2 and y_3 will generate two direction subband coefficients, respectively. In order to discuss the congenetic subband coefficients of the NSCT, just discussing the

decomposition of subband coefficient y_0. y_0 can generate the direction subband coefficients w_0 and w_1.

From the discussion above, the process of the three level direction decomposition on the scale image x is obvious. And then the congenetic subband coefficients of the NSCT is discussed next. The subband coefficients y_0 and y_1 derive from the decomposition of subband coefficient v_0, so y_0, y_1 and v_0 are the congenetic subband coefficients and they have strong relational property when calculating the strong edges, weak edges and noise of subband coefficients y_0 and y_1. The subband coefficients w_0 and w_1 derive from the decomposition of subband coefficient y_0, and then the subband coefficient y_0 derives from the decomposition of subband coefficient v_0, so w_0, w_1, y_0 and v_0 are the congenetic subband coefficients and they have strong relational property when calculating the strong edges, weak edges and noise of subband coefficients w_0 and w_1. As the discussion above, the concept of congenetic subband coefficients is proposed.

4 Adaptive Denoising Theory

4.1 The Entire Relational Correlation Value Among the Congenetic Subband Coefficients of the NSCT

The congenetic subband coefficients of the NSCT have strong relational property. So the strong relational property can be used to calculate the strong edges, weak edges and noise. There are two congenetic subband coefficients s_0 and s_1 which are defined as:

$$s_0 = \{s_0(1,1), s_0(1,2), s_0(1,3), \ldots, s_0(m,n)\} \tag{1}$$

$$s_1 = \{s_1(1,1), s_1(1,2), s_1(1,3), \ldots, s_1(m,n)\} \tag{2}$$

In order to gain the strong relational property data, calculating the initial value that is defined as:

$$\bar{s}_0 = s_0 / |s_0|_{\max} \tag{3}$$

$$\bar{s}_1 = s_1 / |s_1|_{\max} \tag{4}$$

In order to get the relational correlation matrix, calculating the difference value matrix which is defined as:

$$d = \{|s_0(1,1) - s_1(1,1)|, \ldots, |s_0(m,n) - s_1(m,n)|\} \tag{5}$$

Using the difference value matrix of the congenetic subband coefficients of the NSCT, getting the relational correlation matrix of the congenetic subband coefficients s_0 and s_1; the relational correlation matrix ψ is defined as:

$$\psi = (\min(d) + \varepsilon \cdot \max(d))/(d + \varepsilon \cdot \max(d)) \tag{6}$$

where $\min(d)$ may be zero, in order to avoid this phenomenon, we set $\varepsilon = 0.1$, $\varepsilon \in (0, 0.5]$. The parameter ε should be small, and then the strong relational property will be preserved. If the parameter ε is large, the strong relational property will be reduced; and then the amount of strong edges will reduce, the noise amount will increase.

Therefore, the entire relational correlation value of the congenetic subband coefficients of the NSCT is described as follow:

$$\eta = \frac{1}{mn}\sum_{i=1}^{m}\sum_{j=1}^{n}\psi(m,n) \tag{7}$$

η is the entire relational correlation value. In order to calculate the strong edges, weak edges and noise of the congenetic subband coefficients s_0 and s_1 of the NSCT, not only the η value is needed, but also some other value is needed.

4.2 The Grey Correlation Value in Single Coefficient of the NSCT

$s(m,n)$ is the representative of congenetic subband coefficients of the NSCT. The point $s(i,j)$ is in the subband coefficient $s(m,n)$. The window of size 3×3 is used to analyze the point $s(i,j)$. The grey correlation value of the point $s(i,j)$ in every direction can be described as follow:

$$\eth_{h1} = \frac{s(i,j-1)}{s(i,j-1) + |s(i,j) - s(i,j-1)|} \tag{8}$$

$$\eth_{h2} = \frac{s(i,j+1)}{s(i,j+1) + |s(i,j) - s(i,j+1)|} \tag{9}$$

$$\eth_{v1} = \frac{s(i-1,j)}{s(i-1,j) + |s(i,j) - s(i-1,j)|} \tag{10}$$

$$\eth_{v2} = \frac{s(i+1,j)}{s(i+1,j) + |s(i,j) - s(i+1,j)|} \tag{11}$$

$$\eth_{d1} = \frac{s(i-1,j-1)}{s(i-1,j-1) + |s(i,j) - s(i-1,j-1)|} \tag{12}$$

$$\eth_{d2} = \frac{s(i-1,j+1)}{s(i-1,j+1) + |s(i,j) - s(i-1,j+1)|} \tag{13}$$

$$\eth_{d3} = \frac{s(i+1,j-1)}{s(i+1,j-1) + |s(i,j) - s(i+1,j-1)|} \tag{14}$$

$$\eth_{d4} = \frac{s(i+1,j+1)}{s(i+1,j+1) + |s(i,j) - s(i+1,j+1)|} \tag{15}$$

where $\eth_{h1}$ and $\eth_{h2}$ are the grey correlation value of horizontal direction; $\eth_{v1}$ and $\eth_{v2}$ are the grey correlation value of vertical direction; $\eth_{d1}$, $\eth_{d2}$, $\eth_{d3}$ and $\eth_{d4}$ are the grey correlation value of diagonal direction.

$$\eth_{\max} = \max(\eth_{h1}, \eth_{h2}, \eth_{v1}, \eth_{v2}, \eth_{d1}, \eth_{d2}, \eth_{d3}, \eth_{d4}) \tag{16}$$

$$\eth_{\min} = \min(\eth_{h1}, \eth_{h2}, \eth_{v1}, \eth_{v2}, \eth_{d1}, \eth_{d2}, \eth_{d3}, \eth_{d4}) \tag{17}$$

$\eth_{\max}$ and $\eth_{\min}$ are the maximum and minimum grey correlation value on any point of subband coefficient of the NSCT, respectively.

4.3 Adaptive Modifying the Subband Coefficients of the NSCT

As the discussion above, combining the entire relational correlation value among the congenetic subband coefficients of the NSCT with the grey correlation value in the single coefficient of congenetic subband coefficients of the NSCT to calculate the strong edges, weak edges and noise in the single coefficient of congenetic subband coefficients of the NSCT. After the calculation, getting the strong edges, weak edges and noise, the single coefficient that its grey correlation value has been used in this calculation can be modified.

For the every coefficient of L level decomposition, it has L congenetic subband coefficients, so there are C_{L+1}^2 difference value matrix among the $L+1$ congenetic subband coefficients of the NSCT; they are $d_1, d_2, \ldots, d_{C_{L+1}^2}$, respectively; so getting the average difference value matrix:

$$\overline{d} = \frac{1}{C_{L+1}^2} \sum_{i=1}^{C_{L+1}^2} d_i \tag{18}$$

The corresponding relational correlation matrix is shown follow:

$$\overline{\psi} = (\min(\overline{d}) + \varepsilon \cdot \max(\overline{d})) / (\overline{d} + \varepsilon \cdot \max(\overline{d})) \tag{19}$$

So the final entire relational correlation value is defined as follow:

$$\eta = \frac{1}{mn} \sum_{i=1}^{m} \sum_{j=1}^{n} \overline{\psi}(m,n) \tag{20}$$

Getting the final entire relational correlation value, can calculate the strong edges, weak edges and noise in the every single coefficient of the L level decomposition of the NSCT.

The single coefficient $s_l(m,n)$ of L level decomposition of the NSCT has the corresponding final entire relational correlation value η which can be got by the Eq. (20), and at the same time, the same single coefficient $s_l(m,n)$ of L level decomposition of the NSCT also has the corresponding grey correlation value $\partial_{\max}$ and $\partial_{\min}$. Combining $\partial_{\max}$, $\partial_{\min}$ with η to calculate the strong edges, weak edges and noise in the single coefficient $s_l(m,n)$ of L level decomposition of the NSCT, which is described as follow:

If $\partial_{\min} \geq \eta$, then $s_l(i,j)$ is strong edge;
If $\partial_{\max} \leq \eta$, then $s_l(i,j)$ is noise;
If $\partial_{\min} < \eta$ and $\partial_{\max} > \eta$, then $s_l(i,j)$ is weak edge.

Now, the strong edges, weak edges and noise have been known, and then the coefficients $s_l(i,j)$ can be modified. So the coefficients can be modified as follow:

$$s_l(m,n) = \left\{ \begin{array}{ll} s_l(i,j), & \text{if } \partial_{\min} \geq \eta \\ 0, & \text{if } \partial_{\max} \leq \eta \\ 0.1 \cdot \eta \cdot s_l(i,j), & \text{if } \partial_{\min} < \eta \text{ and } \partial_{\max} > \eta \end{array} \right\} \tag{21}$$

As the discussion above, calculating the strong edges, weak edges and noise, and then modifying the subband coefficients of the NSCT. This theory can denoise the image noise and preserve the image edges automatically, which is the adaptive denoising theory that proposed in this paper.

Because the noise image contains noise, leading to the noise image may be discontinuous, which will generate the "Gibbs" phenomenon; in order to eliminate the "Gibbs" phenomenon, the total variation theory [10] is used to process the low-frequency area of the NSCT. And then use the low-frequency area which is processed by total variation and the high-frequency area which is processed by the theory proposed in this paper to reconstruct the image, getting the denoising image. The flow chart of our algorithm is shown in Fig. 6a.

5 Results and Discussion

In this section, combining the adaptive denoising theory with the congenetic subband coefficients of the NSCT in the image denoising, modifying the coefficients of the NSCT, and then using the coefficients that have been modified to reconstruct the image which has been denoised. This is the denoising method proposed by this paper. In recent years, lots of excellent denoising methods have been proposed, and their denoising effect is very great, and these excellent methods should not be the end for the denoising research, so lots of scholars still research the denoising theory further. The non-local means (NL-means) [11] theory is the outstanding denoising method, and many researchers like it very much besides me. This paper will compare the method which proposed by this paper with the NL-means method, through the compare, showing the improvement of our method at certain degree. The PSNR value is chosen as the criterion. If the PSNR value is large, the denoised degree is great.

To test the applicability of our algorithm, the experiment has used many stand images to test and chosen the "lena" as an example. Comparing image-denoising results by experiments on "lena". The direction decomposition level of the NSCT is two on the first residual image. The size of the image "lena" is 512 * 512. The purpose of image-denoising is to get better vision effect in the denoised image. The PSNR value can show if the quality of the image has been improved by the denoising method. From the Fig. 6b, can see that our algorithm has higher PSNR value than NL-means algorithm.

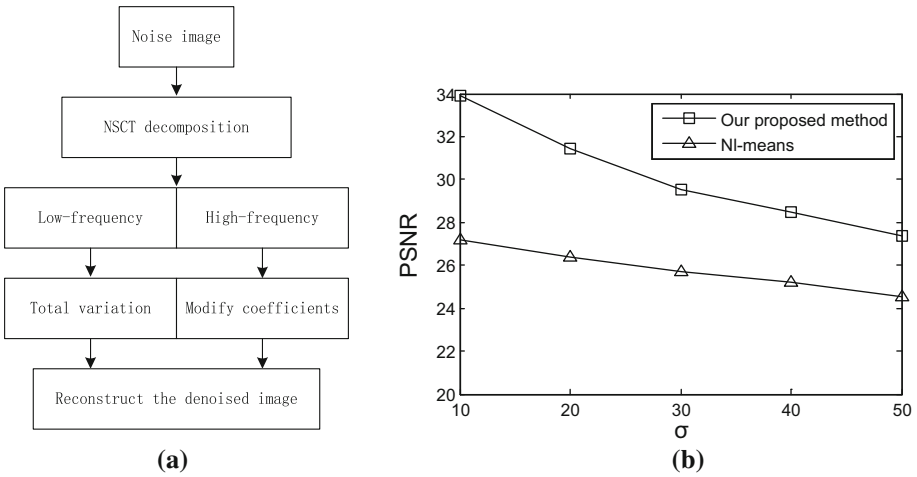

Fig. 6 **a** The proposed algorithm flow chart. **b** The PSNR value of different method

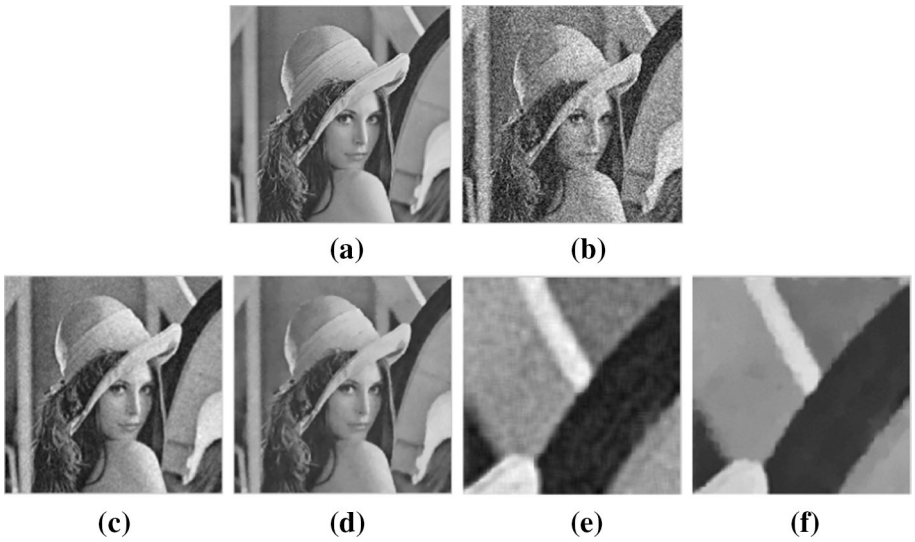

Fig. 7 **a** The original image; **b** the noise image added corresponding Gaussian white noise; **c** the image denoised by NL-means method; **d** the image denoised by our method; **e** the magnifying part of **c**; **f** the magnifying part of **d**

Figure 7c is the image denoised by NL-means method, which still contains noise. Figure 7d is the image denoised by our method, which contains less noise than Fig. 7c. Figure 7e is the local magnifying part of Fig. 7c, and then it shows much noise. Figure 7f is the local magnifying part of Fig. 7d, and then it contains less noise than Fig. 7e, obviously. In order to evaluate the quality of the denoised images, the structure similarity (ssim) [12] is used to calculate the ssim between the original image and every denoised image. If the value of the ssim is large, the denoised image has high similarity with the original image, showing that the denoising result is very good. Through the calculation, the NL-means ($ssim_1 = 0.7136$) in Fig. 7c, and our method ($ssim_2 = 0.8055$) in Fig. 7d. Through the comparison, $ssim_2 > ssim_1$, our method is superior to NL-means method.

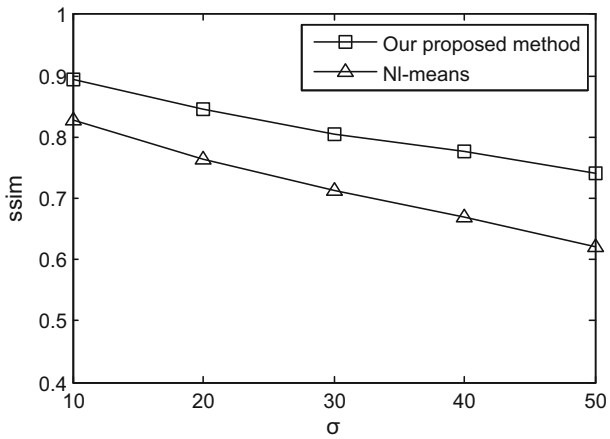

Fig. 8 The ssim value of different methods

Through the calculation, the ssim value of different methods in different standard deviation of noise is gained, which is shown in Fig. 8. Through the comparison, our method can maintain the edges, details and texture characteristics of image; our method has better vision effect. The vision effect is subjective, the effect could be influenced by different observers. So the ssim is used to assess the denoised image with the original image, which objectively supports our algorithm.

6 Conclusion

In this paper, the entire relational correlation value and grey correlation value of congenetic subband coefficients in multiscale and multidirection analysis are researched. Due to the character of fully shift-invariant, multiscale, multidirection and simple implementation, the NSCT is chosen as the decomposition tool. Using the entire relational correlation value and grey correlation value of congenetic subband coefficients of the NSCT to modify the coefficients, so a novel adaptive denoising theory based on the NSCT is proposed. The experiment is conducted to show the applicability of our algorithm and the ability that our algorithm can identify the strong edges, weak edges and noise in the coefficients accurately; and then our method can preserve the edges, details and texture characteristics of the image. Our method is not complex, so it's easy to calculate. For the further research, the congenetic subband coefficients denoising theory will be used to apply in other decomposition tool.

Acknowledgements The authors acknowledge the Fundamental Research Funds for the Central Universities (Grant: 2572018BF05), Special Funds for Scientific and Technological Innovation Talents of Harbin (Grant: 2014RFQXJ127) and Financial assistance from postdoctoral scientific research developmental fund of Heilongjiang Province (Grant: LBH-Q14006).

References

1. Wee, A., Grayden, D., Zhu, Y., et al. (2008). A continuous wavelet transform algorithm for peak detection. *Electrophoresis, 29,* 4215–4225.
2. Pad, Pedram, Alishahi, Kasra, & Unser, Michael. (2017). Optimized wavelet denoising for self-similar alpha-stable processes. *IEEE Transactions on Information Theory, 63*(9), 863–877.
3. Wu, S., Chen, H., Bai, Y., et al. (2015). Remote sensing image noise reduction using wavelet coefficients based on OMP. *Optik-International Journal for Light and Electron Optics, 126*(1516), 1439–1444.
4. Do, M. N., & Vetterli, M. (2005). The Contourlet transform: an efficient directional multiresolution image representation. *IEEE Transactions on Image Processing, 14*(12), 2091–2106.
5. Guo, Q., Dong, F. M., Sun, S. F., et al. (2013). Image denoising algorithm based on contourlet transform for optical coherence tomography heart tube image. *IET Image Processing, 7*(5), 442–450.
6. Cunha, A. L., Zhou, J. P., & Do, M. N. (2006). The nonsubsampled contourlet transform: theory, design and applications. *IEEE Transactions on Image Processing, 15*(10), 3089–3101.
7. Zhou, Y., & Wang, J. (2012). Image denoising based on the symmetric normal inverse Gaussian model and non-subsampled contourlet transform. *IET Image Processing, 6*(8), 1136–1147.
8. Li, H. J., Zhao, Z. M., & Yu, X. L. (2010). A novel image denoising algorithm in wavelet domain using total variation and grey theory. *Engineering Computations, 27*(7), 863–877.
9. Li, H. J., Zhao, Z. M., & Yu, X. L. (2012). Grey theory applied in non-subsampled contourlet transform. *IET Image Processing, 6*(3), 264–272.
10. Dou, Z. Y., Song, M. N., Gao, K., et al. (2017). Image smoothing via truncated total variation. *IEEE Access, 5,* 27337–27344.

11. Karam, Christina, & Hirakawa, Keigo. (2018). Monte-Carlo acceleration of bilateral filter and non-local means. *IEEE Transactions on Image Processing, 27*(3), 1462–1474.
12. Wang, Z., & Bovik, A. C. (2002). A universal image quality index. *IEEE Signal Processing Letters, 9*(3), 81–84.

Peng Wu was born in 1980. He is an associate professor in Northeast Forestry University. He has published nearly 40 academic papers. His main interests include image processing, nonlinear control and Simulation.

Baokun Wang was born in 1990. He is studying for the master degree in the Northeast Forestry University. His main interests include image processing and control of nonlinear system.